SURFZONE EDDIES IN A STRONG ALONGSHORE CURRENT: FORCED OR INSTABILITIES?

Falk Feddersen[1]

Abstract

The surfzone contains energetic two-dimensional (2D) horizontal eddies with length-scale larger than the water depth. These 2D eddies can be generated by both a shear-instability mechanism and by breaking- wave forcing - either at the alongshore length-scale of individual wave breaking (< 20 m) or at wave group length-scales (> 100 m). The dominant surfzone eddy generation mechanism is not understood. The wave- resolving model funwaveC is used to simulate surfzone eddies from 4 cases examples from the SandyDuck field experiment which had alongshore uniform bathymetry. The funwaveC model is initialized with the observed bathymetry and the incident wave field in 8-m depth. The funwaveC model predictions of $E(f,k_y)$ will be compared to the observations. Then, the model vorticity dynamics will be examined to address the question of whether shear-instability or breaking-wave forcing is the dominant eddy generation mechanism. Subsequently, the scales of the alongshore wave forcing will be examined to determine the relative magnitude of vorticity generated by individual short-crested wave breaking (< 20 m) versus wave groups (> 100 m).

1. Introduction

The surfzone is a place of energetic two-dimensional (2D) horizontal turbulent eddies with length-scales greater than the water depth. A signature of surfzone eddies is transient rip currents (as opposed to bathymetrically controlled rip currents) which are easily visualized in surfzone dye release experiments (Figure 1). These eddies have rotational (as opposed to irrotational) velocities which are associated with vertical vorticity (hereafter termed vorticity). Recent surfzone dye tracer observations and modeling indicate that absolute cross-shore diffusivity on an alongshore uniform beach, is related to the bulk (surfzone-averaged) rms horizontal rotational velocities (Clark et al., 2010, 2011). Drifter-derived time-dependent absolute cross-shore diffusivities were consistent with stirring due to surfzone eddies with Lagrangian (not Eulerian) time-scales of O(100) s (Spydell and Feddersen, 2012b). When alongshore current shear was strong, drifter-derived alongshore diffusivities were well-predicted by a shear-dispersion theory that includes non-zero Lagrangian time-scale (Spydell and Feddersen, 2012a). Thus, 2D surfzone eddies are responsible for dispersion and dilution of surfzone tracers on alongshore uniform beaches. On rip-channeled (not alongshore uniform) beaches, dispersion may occur due to both 2D eddies and mean circulation features (e.g., Johnson and Pattiaratchi, 2004; Brown et al., 2009).

Time-dependent 2D eddies within the surfzone were first identified as a low-frequency, non-dispersive ridge in frequency (f) and alongshore-wavenumber (k_y) velocity spectra $E(f,k_y)$ outside of the gravity wave region (Oltman-Shay et al., 1989) – see Figure 2,right. These motions have variability on Eulerian time-scales between 50–500 s, alongshore length-scales between 40-250 m, and $E(f,k_y)$ ridge slopes are approximately equal to the mean alongshore current V (e.g., Oltman-Shay et al., 1989; Noyes et al., 2004). The magnitude of these eddies was also generally related to V (Noyes et al., 2004). However, even during times of weak V, surfzone eddies are observed. For example, on a monotonic alongshore uniform beach with $V = 0$ m s^{-1}, the presence of a scale-dependent relative diffusivity indicated the presence of an energetic eddy field with scales varying from 5-50 m (Spydell et al., 2007; Spydell and Feddersen, 2009). During times of weak $|V|$ (< 0.25 ms^{-1}), eddies (rotational velocity outside of the gravity wave region) were observed with eddy velocities of up to 0.1-0.2 m s^{-1} (MacMahan et al., 2010).

[1]Scripps Institution of Oceanography, La Jolla CA 92093-0209 USA, falk@coast.ucsd.edu

Figure 1: Aerial photograph of the surfzone and beach (at the top) at the alongshore uniform Imperial Beach CA during a IB09 experiment Rhodamine dye release. The signature of eddies within the surfzone is evident as they generate transient rip currents ejecting dye offshore. (Photo: David Clark)

With linear stability analysis, these motions were associated with the intrinsic generation mechanism of a shear-instability of the alongshore current (e.g., Bowen and Holman, 1989; Dodd et al., 1992, and many others), and thus dubbed “shear-waves”. Shear-instabilities of the mean alongshore current, in particular their nonlinear equilibration, have been studied with nonlinear shallow-water equation (NSWE) with steady wave forcing both numerically (e.g., Allen et al., 1996; Slinn et al., 1998; Özkan and Kirby, 1999; Noyes et al., 2004) and analytically (Feddersen, 1998). NSWE model derived $E(f,k_y)$ reproduced the overall ridge-slope of the observed $E(f, k_y)$ (Özkan and Kirby, 1999; Noyes et al., 2005) - see Figure 2. However, as discussed in Noyes et al. (2005), the model energy generally is concentrated at lower f-k_y, is less broad than observed, and often under-predicts the overall variance (Figure 2).

Vorticity associated with 2D surfzone eddies also is generated through the extrinsic mechanism of short- crested breaking-wave vorticity forcing due to along-crest variation in wave dissipation (Peregrine, 1998). Recently, changes in vorticity with the passage of individual short-crested breaking waves was observed at 10+ m length-scales (Clark et al., 2012), consistent with the theory of Peregrine (1998). The effect of alongshore non-uniform wave breaking on vorticity is seen by taking the curl of the horizontal momentum equation which results in an equation for vorticity ω, e.g.,

$$\partial \omega / \partial t + \ldots = \nabla \times F_{br} + \ldots \tag{1}$$

where F_{br} is the breaking-wave force and . . . represents the remaining terms in the vorticity equation. To see how this term acts as a vorticity source, consider normally incident waves with alongshore varying amplitude. As these waves enter the surfzone, depth-limited breaking only occurs where the waves are largest thus resulting in finite crest-length broken waves and non-zero F_{br} (see schematic in Fig. 3). In this case, F_{br} is cross-shore (x) oriented and varies in the alongshore direction, thus $\nabla \times F_{br}$ is non-zero, generating vorticity.

On alongshore uniform beaches, along-crest variation is due directional spread σ_θ (Kuik et al., 1988) in the incident waves. The larger σ_θ the shorter the average breaking crest length. Wave resolving (WR) models, such a Boussinesq models (e.g., Chen et al., 2003; Feddersen et al., 2011) generate vorticity by this mechanism. Surfzone vorticity, and hence tracer dispersion, should then depend upon the incident wave directional spread $\sigma_{\theta 0}$. Indeed, on an alongshore uniform beach with bulk-mean normally incident waves and constant incident wave energy, the surfzone averaged rms vorticity increases with increasing wave directional spread (Spydell and Feddersen, 2009) – see Figure 4.

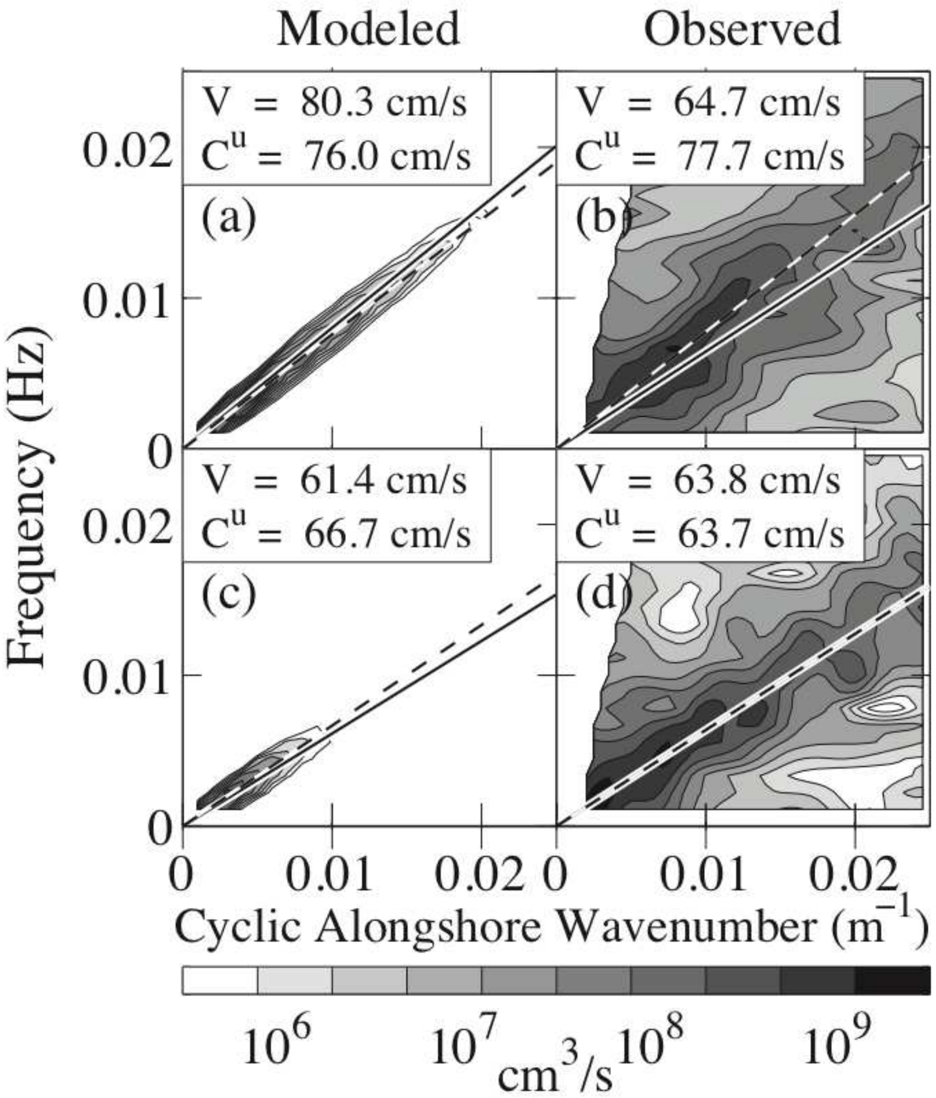

Figure 2: Example SandyDuck experiment cross-shore velocity alongshore-wavenumber-frequency spectra *E(f,k$_y$)* for NSWE modeled (left) and observed (right) at cross-shore locations (a,b) within and (c,d) seaward of the surfzone. The gravity wave region bounded by the mode zero edge wave dispersion is blanked out to the left of panels (b) and (d). The local mean alongshore current *V* (solid line) and best-fit shear wave phase speed C_u (dashed line) are given in the legend. (from Noyes et al., 2005)

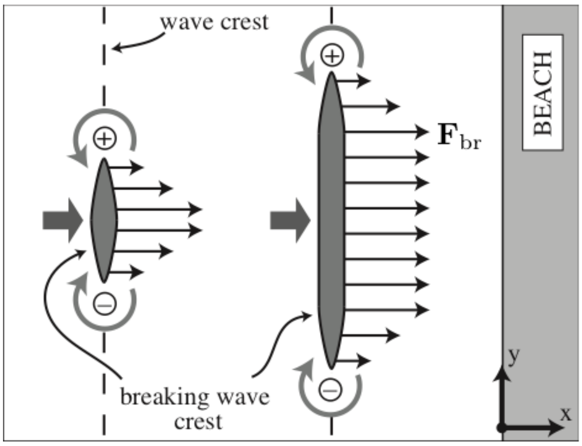

Figure 3: Simplified schematic of finite breaking crest length vorticity generations. Normally-incident finite crest-length breaking waves approach the beach and the breaking crest-length gets longer closer to the beach. The Boussinesq model breaking-wave force F_{br} is cross-shore oriented and is alongshore variable. This results in a non-zero $\nabla \times F_{br}$ generating positive and negative vorticity at the crest-ends (e.g., Peregrine, 1998). (from Spydell and Feddersen, 2009)

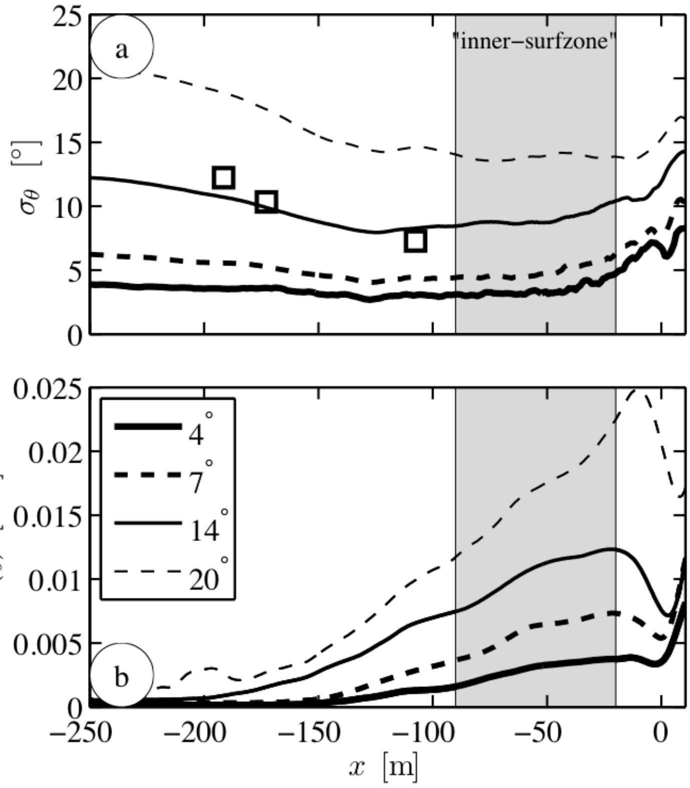

Figure 4: Modeled (a) wave directional spread σ_θ and (b) vorticity standard deviation std(ζ) versus x for different incident directional spreads $\sigma_{\theta 0}$. The open squares in (a) are the ADV observations. (from Spydell and Feddersen, 2009)

Because the length-scale of horizontal surfzone eddies is much larger than the water depth, the dynamics of surfzone eddies likely follow those of 2D turbulence (e.g., Kraichnan and Montgomery, 1980; Tabeling, 2002; Boffetta and Ecke, 2012). A basic principle of (both freely-decaying and forced) 2D turbulence is that eddy energy cascades to longer length-scales through nonlinear interactions. Therefore, vorticity injected at short scales of 10+ m would evolve to larger length-scales creating a rich wavenumber spectrum of surfzone eddies.

Surfzone vorticity can also be generated at the much larger alongshore length-scales of wave-groups, generally O(200 m), by alongshore variation of radiation stress gradients associated with the slow time and slow alongshore evolution of the wave envelope (wave groups) (e.g., Reniers et al., 2004; Long and Özkan Haller, 2009). On alongshore uniform beaches, wave-averaged (WA) models with wave-group forcing can generate very low frequency (VLF, < 0.004 Hz) rotational motions that have alongshore length scales ≈ 200 m or longer (Reniers et al., 2004). The alongshore length-scale of wave groups are related to the k_y width of the incident wave field. Using an example from MacMahan et al. (2010), a deep-water bi-chromatic wave train with with f = 0.1 Hz and angle separation of $\Delta\theta = 25^{\circ}$ gives rise to an alongshore group scale of 200 m. WA models with wave-group forcing have been successful in reproducing VLF eddy energy on rip-channeled beaches (Reniers et al., 2007, 2009). When $V \approx 0$ m s^{-1} and a shear-instability is not possible, modeled surfzone VLF eddy velocities, simulated with a linear (WA) wave-group model, were correlated with observations but overpredicted by 40% (MacMahan et al., 2010). However, as 2D turbulence cascades eddy energy to longer length-scales, wave group forcing cannot generate eddies at the shorter scales that have been observed (Spydell et al., 2007).

Whether shear instabilities or vorticity generated by wave breaking is the more important term in generating surfzone eddies remains an open question. In addition, the relative importance of short-crested (O(10) m scales) versus wave group (O(200) m scales) vorticity forcing in generating surfzone eddies is not well understood. For an idealized surfzone with an "unstable" alongshore current, Long and Özkan Haller (2009) found that vorticity generated by shear instabilities and by wave group forcing contributed approximately equally to a surfzone averaged squared potential vorticity dynamics. However, the shorter scales of vorticity injection by individual breaking waves were not included, and the model was not compared to field observations. Observations of surfzone eddies with strong V have not been directly compared to a model that includes both the intrinsic shear-instability mechanism and extrinsic wave forcing (short-crested or wave groups) mechanisms.

The WR Boussinesq model funwaveC will be used to diagnose the relative importance of the intrinsic shear-instability mechanism and the extrinsic (short-crested or wave-group) wave breaking mechanism in generating surfzone eddies. Four case examples from the SandyDuck field experiment, where observed $E(f,k_y)$ spectra were compared to a results from a NSWE model with steady forcing Noyes et al. (2005), are simulated with funwaveC. The funwaveC model is initialized with the observed bathymetry and the incident directional wave field in 8-m water depth. The ability of the model to reproduce observed $E(f,k_y)$ spectra will be examined. In addition, the model vorticity dynamics will be diagnosed. This will lead to an answer of the question in the title.

2. SandyDuck Surfzone Observations

Observations were collected as part of the SandyDuck experiment that took place in Aug-Nov 1997 at the Army Corp of Engineers Field Research Facility (FRF) in Duck NC. The observations are described in detail elsewhere (Elgar et al., 2001; Feddersen and Guza, 2003; Noyes et al., 2002, 2004) and are briefly discussed here. The FRF coordinate system is used where x is the cross-shore coordinate increasing offshore with the shoreline near x = 110 m and y is the alongshore coordinate. A dense cross-shore array of co-located pressure gauges and current meters (PUV) were deployed at 11 locations on a cross-shore transect extending from the shoreline to 5.5 m water depth to measure cross-shore wave and current transformation. In addition, five alongshore arrays (denoted A1-A5 from closest to farthest from shore) of PUV were deployed (Figure 5) to measure $E(f,k_y)$ for both cross- (u) and alongshore (v) velocities using an iterative maximum likelihood estimator (Noyes et al., 2002, 2004). A pressure sensor array in 8-m water depth provides incident wave statistics including wave spectra, mean wave-angle, and directional spread $\sigma_\theta(f)$ (Kuik et al., 1988). Wind stress τ_w was estimated from measurements at the end of the FRF pier. Observations of surfzone eddies during the 4-month-long SandyDuck experiment are described by Noyes et al. (2004) and MacMahan et al. (2010). Using a NSWE model with steady forcing, Noyes et al. (2005) simulated four, 3-hr-long case examples, 28 Aug (0828), 1 Nov (1101), 13 Nov (1113), and 17 Nov (1117), that are also simulated here. The bathymetry and mean circulation in the instrumented area usually was alongshore homogeneous (Feddersen and Guza, 2003), although alongshore variability of V at the shallowest array A1 was significant on 1101 and 1113.

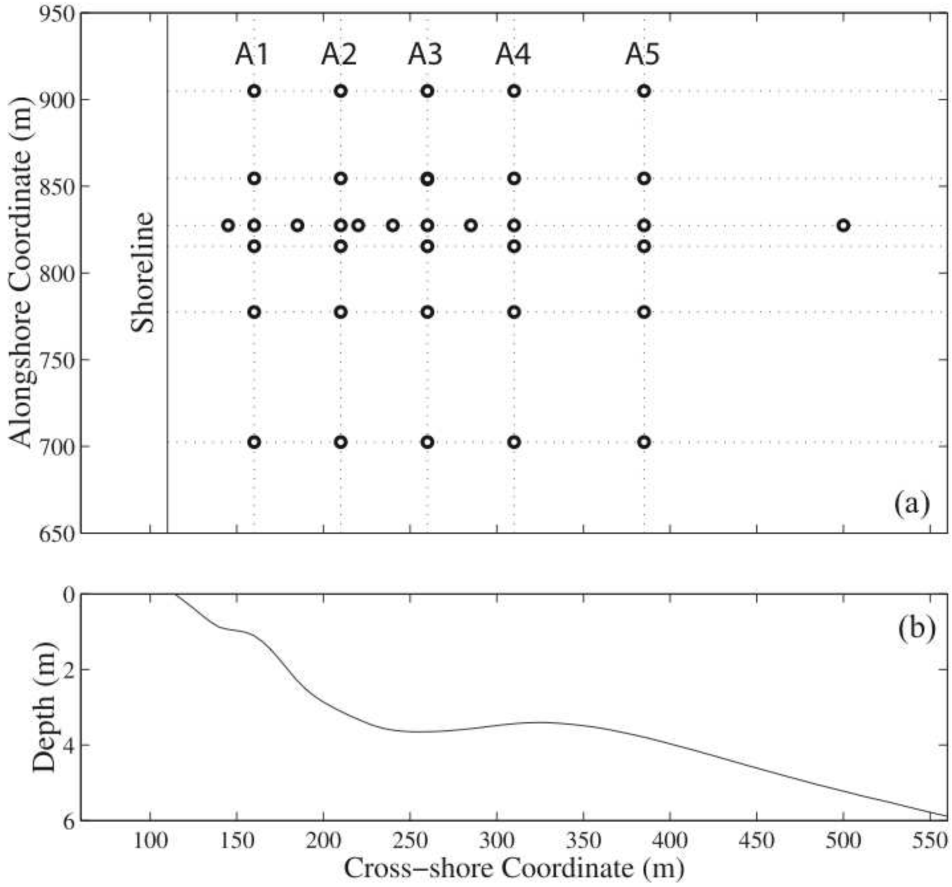

Figure 5: (a) Plan view of SandyDuck instrument array. Each circle indicates a velocity sensor. The Field Research Facility coordinate system is used where (x, y) are cross- and alongshore, respectively. The five alongshore arrays are indicated A1–A5. The approximate location of the shoreline is shown near x = 110 m. (b) Alongshore-averaged depth below mean sea level versus cross-shore coordinate.

3. Wave-resolving Boussinesq model funwaveC

The open-source, wave-resolving Boussinesq model funwaveC has been previously used to study a variety of surfzone processes including: cross-shore tracer dispersion driven by individual bores (Feddersen, 2007), surfzone drifter dispersion in a weak alongshore current (Spydell and Feddersen, 2009), spectral wave transformation, mean currents, and surfzone eddies (Feddersen et al., 2011), cross-shore tracer dispersion in moderate alongshore currents (Clark et al., 2011), shoreline runup (Guza and Feddersen, 2012), and net circulation cells on coral reef spur and groove formations (Rogers et al., 2013). Additional details are found elsewhere (Feddersen et al., 2011).

The alongshore uniform model bathymetry is based on those used by Noyes et al. (2005) with an additional offshore 200 m wide region of constant depth between 7–8 m depth and a sub-aerial beach extending to 2–2.4 m above mean sea level, depending upon the case example, to allow runup. The constant depth region contains the wavemaker and a 90-m offshore sponge layer that absorbs seaward propagating waves. Shoreline runup is implemented using the “thin-layer” method (Salmon, 2002). The total cross-shore domain is near 870 m for all case examples. The cross- and alongshore grid sizes are 1 m and 1.25 m, respectively. The alongshore domain width is 1500 m with alongshore periodic boundary conditions.

A wavemaker (Wei et al., 1999), located immediately onshore of the offshore sponge layer, approximately generates the target frequency-directional spectrum based upon the wave spectra, mean wave angle and $\sigma_\theta(f)$ observed in 8-m water depth. Full details of the model wavemaker are given in Feddersen et al. (2011). The model wavemaker is forced at many randomly-spaced discrete frequencies between $0.06 < f < 0.25$ Hz at an average frequency resolution of 0.0004 Hz. The randomly spaced frequencies makes the wavemaker recurrence much longer than the model simulation. The realistic modeled incident directional wave field allows for vorticity generation at the short length-scales of individual short-crested breaking waves and the longer wave group scales.

For each case example, the model was run for 8000 s and model output is analyzed over the last 5000 s. The 3000 s allowed for model spinup was sufficient for mean-square vorticity to equilibrate similar to other surfzone simulations (Feddersen et al., 2011). Example model snapshot of instantaneous sea-surface elevation and vorticity are shown in Figure 6. Modeled frequency-dependent wave spectral quantities and "bulk" sea-swell band wave quantities such as significant wave height H_s are calculated with the same estimation methods as the field observations.

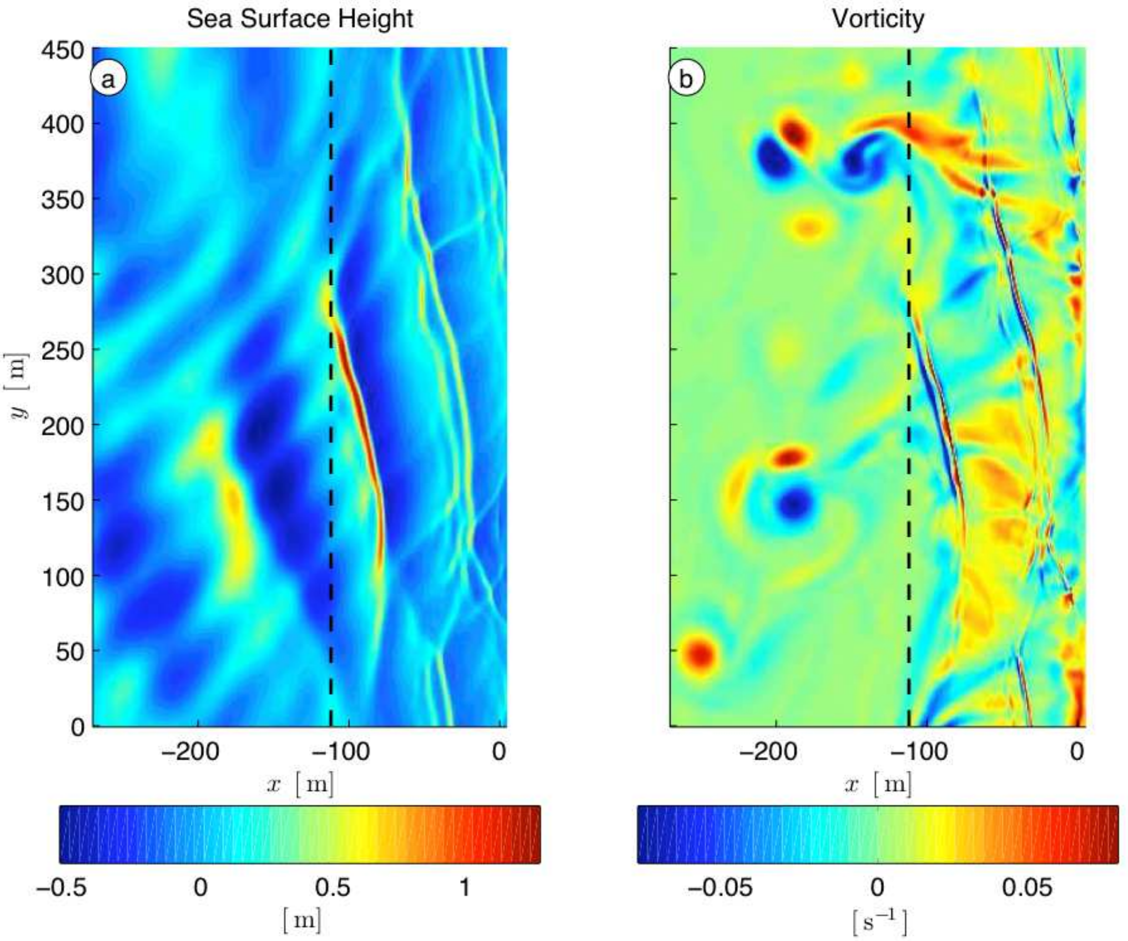

Figure 6: Example snapshot in time of modeled (a) sea surface elevation η, and (b) vorticity ζ versus x and y. The shoreline is located at x = 0 m and the black dashed line is the approximate outer limit of the surfzone. Note the broad range of vorticity length-scales within the surfzone. (from Feddersen et al., 2011)

4. Results: Model-data comparison

As a precondition to testing the model's ability to accurately simulate the surfzone eddy field, model data comparison will be first performed for bulk parameters such as significant wave height H_s and mean alongshore current V. Subsequently, the funwaveC model derived frequency-alongshore wavenumber spectra $E(f,k_y)$ will be compared to the observed and NSWE modeled $E(f,k_y)$ reported in Noyes et al. (2005) at alongshore arrays within and seaward of the surfzone. The NSWE with steady wave forcing only generates eddies via the intrinsic shear-instability mechanism, whereas the wave-resolving funwaveC also allows eddy generation through both short-crested and wave-group breaking-wave vorticity generation mechanism.

The $E(f,k_y)$ comparison will also be made quantitative by comparing the rotational velocities u_{rot} and v_{rot} associated with these $E(f,k_y)$ across all case example days within and seaward of the surfzone. Observed, NSWE modeled, and funwaveC modeled root-mean-square rotational (i.e., vortical) velocities u_{rot} and v_{rot} will be calculated by integrating the respective $E(f,k_y)$ over the non-gravity wave region between f = 0.00165 Hz and f = 0.25 Hz and over alongshore wavenumber k_y outside of the gravity wave region and taking a square root (see Noyes et al., 2004, for processing details). This procedure removes irrotational infragravity wave energy, leaving only rotational (eddy) velocity contributions.

5. Results: Vorticity

If the funwaveC model reproduces the observed surfzone eddy field, then the funwaveC model can be used to diagnose the dominant processes generating surfzone eddies. Vorticity ω and perturbation vorticity ω′ are the natural variables to diagnose competing surfzone eddy generation mechanisms as they corresponds only the (rotational) eddies and not the (irrotational) infra-gravity wave motions.

To diagnose the relative importance of shear instabilities or breaking-wave vorticity forcing to the surfzone eddy field, the mean square perturbation vorticity $\langle \omega'^2 \rangle$ (where the overbar represents an average) is examined. Beginning with the shallow-water based vorticity equation, removing the mean, and multiplying by ω′ and averaging yields the $\langle \omega'^2 \rangle$ evolution equation (e.g., Salmon, 1998),

$$(1/2)\, \partial \langle \omega'^2 \rangle / \partial t + ... = - \langle \omega' u' \rangle dV/dx + \langle \omega' \nabla \times Fbr' \rangle + ... \qquad (2)$$

where the first and second terms on the right-hand side of (2) are the shear-instability and breaking-wave contributions, respectively. Other terms not shown in (2) are the advection and stretching terms that transform but to not generate eddies, and the bottom-friction induced $\langle \omega'^2 \rangle$ decay. The relative magnitudes of the breaking wave $\langle \omega'^2 \rangle$ forcing to the shear instability term ($\langle \omega' u' \rangle dV/dx$) gives insight into whether the rotational energy (eddies) observed in the $E(f, k_y)$ is due to breaking waves or shear instabilities.

A subsequent consideration is whether the breaking wave vorticity forcing is dominated by the small (≈ 10 m) scales of individual breaking waves (Peregrine, 1998; Clark et al., 2012) or at the larger (≈ 200 m) alongshore length-scales of wave groups. This question can be addressed by examining the cross-surfzone averaged (indicated with a hat) alongshore wavenumber spectra of the breaking-wave vorticity forcing $E_{\nabla \times Fbr}(k_y)$ and the vorticity $E_{\omega}(k_y)$.

6. Acknowledgements

This work was funded by the National Science Foundation and the Office of Naval Research. ONR funded the SandyDuck field experiment. S. Elgar, T. H. C. Herbers, R. T. Guza, and B. Raubenheimer were PIs on the PUV array component of the experiment used here. The instruments were were deployed and maintained by staff from the Center for Coastal Studies, Scripps Institution of Oceanography. Staff from the U.S. Army Corps of Engineers Field Research Facility, Duck, North Carolina, provided processed survey data and data from their pressure array in 8-m water depth. The open source funwaveC model was developed by F. Feddersen is available at http://falk.ucsd.edu.

7. References

Allen, J., P. A. Newberger, and R. A. Holman, 1996: Nonlinear shear instabilities of alongshore currents on plane beaches. *J. Fluid Mech*., 310, 181–213.

Boffetta, G., and R. E. Ecke, 2012: Two-Dimensional Turbulence. *Ann. Rev. Fluid Mech*., 44, doi:10.1146/annurev-fluid-120710-101240, 427–451.

Bowen, A. J., and R. A. Holman, 1989: Shear instabilities of the mean longshore current 1. theory. *J. Geophys. Res.*, 94, 18,023–18,030.

Brown, J., J. MacMahan, A. Reniers, and E. Thornton, 2009: Surf zone diffusivity on a rip-channeled beach. *J. Geophys. Res*., 114, doi:10.1029/2008JC005158.
Chen, Q., J. T. Kirby, R. A. Dalrymple, S. Fengyan, and E. B. Thornton, 2003: Boussinesq modeling of longshore currents. *J. Geophys. Res., Oceans*, 108, doi: 10.1029/2002JC001308.
Clark, D. B., S. Elgar, and B. Raubenheimer, 2012: Vorticity generation by short-crested wave breaking. *Geophys. Res. Lett*., 39, doi:10.1028/2012GL054034.
Clark, D. B., F. Feddersen, and R. T. Guza, 2010: Cross-shore surfzone tracer dispersion in an alongshore current. *J. Geophys. Res*., 115, doi:10.1029/2009JC005683.
— 2011: Modeling surfzone tracer plumes, part 2: Transport and dispersion. *J. Geophys. Res*., Oceans, 116, doi:10.1029/2011JC007211.
Dodd, N., J. Oltman-Shay, and E. B. Thornton, 1992: Shear instabilities in the longshore current: A comparison of observation and theory. *J. Phys. Ocean*., 22, 62–82.
Elgar, S., R. T. Guza, W. C. O'Reilly, B. Raubenheimer, and T. H. C. Herbers, 2001: Wave energy and direction observed near a pier. *J. Waterw. Port Coastal Ocean Eng*., 127, 2–6.
Feddersen, F., 1998: Weakly nonlinear shear waves. *J. Fluid Mech*., 372, 71–91.
Feddersen, F., 2007: Breaking wave induced cross-shore tracer dispersion in the surfzone: Model results and scalings. *J. Geophys. Res.*, 112, doi:10.1029/2006JC004006.
Feddersen, F., D. B. Clark, and R. T. Guza, 2011: Boussinesq modeling of surfzone tracer plumes, Part 1: Eulerian wave and current comparisons. *J. Geophys. Res*., 116, doi:10.1029/2011JC007210. Feddersen, F., and R. T. Guza, 2003: Observations of nearshore circulation: Alongshore uniformity. *J. Geophys. Res*., 108, doi:10.1029/2001JC001293, 6–1.
Guza, R. T., and F. Feddersen, 2012: Effect of wave frequency and directional spread on shoreline runup. *Geophys. Res. Lett*., 39, doi:10.1029/2012GL051959.
Johnson, D., and C. Pattiaratchi, 2004: Transient rip currents and nearshore circulation on a swell-dominated beach. *J. Geophys. Res*., 109, doi: 10.1029/2003JC001798.
Kennedy, A. B., Q. H. Chen, J. T. Kirby, and R. A. Dalrymple, 2000: Boussinesq modeling of wave transformation, breaking and runup I: One dimension. *J. Waterway, Port, Coastal, and Ocean Eng*., 126, 39–47.
Kraichnan, R., and D. Montgomery, 1980: Two-dimensional turbulence. *Reports on Progress in Physics*, 43, doi:10.1088/0034-4885/43/5/001, 547–619.
Kuik, A. J., G. P. V. Vledder, and L. H. Holthuijsen, 1988: A method for the routine analysis of pitch-and-roll buoy wave data. *J. Phys. Ocean*., 18, 1020–1034.
Long, J. W., and H. T. Özkan Haller, 2009: Low-frequency characteristics of wave group–forced vortices. *J. Geophys. Res*., 114.
Lynett, P., 2006: Nearshore modeling using high-order boussinesq equations. *J. Waterway, Port, Coastal, and Ocean Engineering*, 132, 348–357.
MacMahan, J. H., A. J. H. M. Reniers, and E. B. Thornton, 2010: Vortical surf zone velocity fluctuations with 0(10) min period. *J. Geophys. Res*., 115, doi:10.1029/2009JC005383. Noyes, T. J., R. T. Guza, S. Elgar, and T. H. C. Herbers, 2004: Field observations of shear waves in the surfzone. *J. Geophys. Res*., 109, doi:10.1029/2002JC001761.
Noyes, T. J., R. T. Guza, F. Feddersen, S. Elgar, and T. H. C. Herbers, 2005: Model-data comparisons of shear waves in the nearshore. *J. Geophys. Res*., 110, C05019.
Noyes, T. J. A., R. T. Guza, S. Elgar, and T. H. C. Herbers, 2002: Comparison of methods for estimating nearshore shear wave variance. *J. Atmos. and Ocean. Tech*., 19, 136–143.
Nwogu, O., 1993: Alternative form of boussinesq equations for nearshore wave propagation. *J. Wtrwy., Port, Coast., and Oc. Engrg.*, 119, 618–638.
Oltman-Shay, J., P. A. Howd, and W. A. Birkemeier, 1989: Shear instabilities of the mean longshore current 2. Field observations. *J. Geophys. Res*., 94, 18031–18042.
Özkan, H. T., and J. Kirby, 1999: Nonlinear evolution of shear instabilities of the longshore current: A comparison of observations and computations. *J. Geophys. Res., Oceans*, 104, 25,953–25,984.
Peregrine, D. H., 1998: Surf zone currents. *Theor. Comput. Fluid Dyn*., 10, 295–309.
Reniers, A., J. Roelvink, and E. Thornton, 2004: Morphodynamic modeling of an embayed beach under wave group forcing. *J. Geophys. Res*., 109, doi:10.1029/2002JC001586.
Reniers, A. J. H. M., J. H. MacMahan, E. B. Thornton, and T. P. Stanton, 2007: Modeling of very low frequency motions during RIPEX. *J. Geophys. Res*., 112, doi:10.1029/2005JC003122, 3161–3172.
Reniers, A. J. H. M., J. H. MacMahan, E. B. Thornton, T. P. Stanton, M. Henriquez, J. W. Brown, J. A. Brown, and E. Gallagher, 2009: Surf zone surface retention on a rip-channeled beach. *J. Geophys. Res.*, 114, doi:10.1029/2008JC005153.
Rogers, J.S., S.G. Monismith, F. Feddersen, and C. Storlazzi, 2013: Hydrodynamics of Spur and Groove Formations on a Coral Reef. *J. Geophys. Res*., in press.
Salmon, R., 1998: *Lectures On Geophysical Fluid Dynamics*. Oxford University Press, New York, 378 pp.
— 2002: Numerical solution of the two-layer shallow water equations with bottom topography. *J. Mar. Res*., 60, 605–638.
Slinn, D., J. Allen, P. Newberger, and R. Holman, 1998: Nonlinear shear instabilities of alongshore currents over

barred beaches. *J. Geophys. Res*., 103, 18357–18379.
Spydell, M., F. Feddersen, R. T. Guza, and W. E. Schmidt, 2007: Observing surfzone dispersion with drifters. *J. Phys. Ocean*., 27, 2920–2939.
Spydell, M. S., and F. Feddersen, 2009: Lagrangian drifter dispersion in the surf zone: Directionally spread, normally incident waves. *J. Phys. Ocean*., 39, 809–830.
— 2012a: The effect of a non-zero Lagrangian time-scale on bounded shear dispersion. *J. Fluid Mech.*, 691, doi:10.1017/jfm.2011.433, 69–94.
— 2012b: A Lagrangian stochastic model of surfzone drifter dispersion. *J. Geophys. Res*., 117, doi:10.1029/2011JC007701.
Tabeling, P., 2002: Two-dimensional turbulence: A physicist approach. *Physics Reports-Review Section of Physics Letters*, 362, doi:10.1016/S0370-1573(01)00064-3, 1–62.
Wei, G., J. T. Kirby, and A. Sinha, 1999: Generation of waves in Boussinesq models using a source function method. *Coastal Eng*., 36, 271–299.